Observation of nonequilibrium behavior near the Lifshitz point in ferroelectrics with incommensurate phase

K. Z. Rushchanskii[*]

Peter Grünberg Institut, Forschungszentrum Jülich and JARA, D-52425 Jülich, Germany

A. Molnar, R. Bilanych, R. Yevych, A. Kohutych, and Yu. M. Vysochanskii

Institute for Solid State Physics and Chemistry, Uzhgorod National University, 54 Voloshyn St., 88000 Uzhgorod, Ukraine

V. Samulionis and J. Banys

Physics Faculty, Vilnius University, Sauletekio al. 9/3, 10222 Vilnius, Lithuania

We have investigated nonequilibrium properties of proper uniaxial $Sn_2P_2(Se_xS_{1-x})_6$ ferroelectrics with the type II incommensurate phase above Lifshitz point $x_{LP} \sim 0.28$. We performed measurements of dielectric susceptibility in cooling and heating regimes with the rate ranging 0.002–0.1 K/min, as well as high-resolution ultrasound investigation and hypersound Brillouin scattering experiments. For samples with $x \geqslant 0.28$ clear anomalies are observed at incommensurate second-order transition (T_i) and at first-order lock-in transition (T_c) in the regime of very slow cooling rate, whereas the intermediate incommensurate phase is not observed when the rate is faster than 0.1 K/min. In general, increasing the cooling rate leads to smearing of the anomaly at T_c. We relate this effect to cooling rate dependence of domain-wall concentration and their size: domain width decreases when cooling rate increases. At certain conditions, the size of domain is comparable to the incommensurate phase modulation period, which is in the micrometer range in the vicinity of Lifshitz point and leads to pinning of the modulation period by domain walls.

I. INTRODUCTION

Multiferroic properties and functionality of nanosized objects are related to inhomogeneous space distribution of the order parameters close to the surface and to competitive interactions in the bulk of materials. This could lead to exotic domain structures [1] and/or to modulation waves in periodic polarization arrangement [2,3] below phase transition (PT) temperature (i.e., in polar phase). Strong nonlinearity of the local potential could determine the peculiar shape of domain walls and their temperature evolution in ferroelectric phase [4–6]. When domain dimension starts to be comparable with modulation wavelength in the incommensurate phase (IC), one could expect their interference leading to new interesting phenomena. In materials with the Lifshitz point [7–9] (LP, see following) in their compositional (or pressure) temperature phase diagrams the modulation period could be changed continuously. This makes them good candidates to study such interference. Subsequently, interesting phenomena could appear by transformation of domain structure into IC modulation across lock-in transition near the LP.

Such possibilities could be investigated in the unique case of $Sn_2P_2(Se_xS_{1-x})_6$ mixed crystals [9]. From one side, sulphide $Sn_2P_2S_6$ (SPS) is a proper uniaxial ferroelectric with the second-order PT at $T_0 \sim 337$ K from monoclinic $P2_1/c$ paraelectric phase to Pc ferroelectric one. Strongly nonlinear local potential for the polarization fluctuations determines mixed displacive-order-/-disorder nature of this PT [10–12]. Corresponding isostructural selenide $Sn_2P_2Se_6$ has IC phase

between second-order transition at $T_i \sim 221$ K and first-order lock-in transition at $T_c \sim 193$ K. In pure $Sn_2P_2Se_6$, the IC phase has modulation period about 14 elementary cells [13,14]. In mixed $Sn_2P_2(Se_xS_{1-x})_6$ compounds the IC phase appears at $x > x_{LP} \sim 0.28$, where the x_{LP} denotes the LP concentration on the $T - x$ diagram [9,15,16]. In this case, LP is a triple point between paraelectric, ferroelectric, and incommensurate phase in composition phase diagram. A characteristic feature of the LP point is that modulation period increases continuously with concentration x of Se, starting from zero at the position of x_{LP}. The mean field theory of the LP with one component order parameter and one direction of modulation [8] predicts that both modulation wave number q_i and temperature range of the IC phase $T_i - T_c$ changes as $q_i \sim (x - x_{LP})^{0.5}$ and $T_i - T_c \sim (x - x_{LP})^2$, correspondingly. The LP demonstrates a new universality class for critical anomalies of thermodynamic properties [7]. The critical behavior is different in the case of uniaxial ferroelectrics [17] (uniaxial Lifshitz point, ULP) and in the case of coincidence with position of tricritical point (uniaxial tricritical Lifshitz point, UTLP) [18–20].

On a microscopic level, the IC phase and LP diagram could be described in axial next-nearest-neighbor interaction (ANNNI) model [21], which accounts for the ratio between strength of nearest- and next-nearest interactions. For the $Sn_2P_2Se_6$ compound it was found that substitution of sulfur by selenium increases the chemical bond's covalence [22,23] and, therefore, rearranges the intercell interactions. In the phonon spectra this replacement leads to decrease of the LO-TO splitting for the lowest-energy polar soft mode and to strengthening of linear interaction of the soft optic and acoustic phonons, which are polarized in the monoclinic symmetry plane [24]. An *ab initio* model of phase transition in $Sn_2P_2S_6$ crystals

_____
[*]k.rushchanskii@fz-juelich.de

[4] revealed that strong coupling between low-energy polar and full-symmetry modes leads to ferroelectric instability in $Sn_2P_2S_6$ class of materials.

Phenomenological theory of ferroelectrics with type II IC phase, which includes the Lifshitz-type invariant in the Landau thermodynamic potential and accounts for the inhomogeneous interaction of the spontaneous polarization with deformations, was developed in Refs. [25–27]. Experimentally, such interaction could be observed as linear coupling of the soft optic and acoustic branches and have been studied by neutron scattering for $Sn_2P_2S_6$ and $Sn_2P_2Se_6$ crystals [14,28]. This interaction was also observed in $Sn_2P_2(Se_xS_{1-x})_6$ mixed crystals near the LP, where clear evidence of the simultaneous softening of longitudinal and transverse acoustic branches have been established in Brillouin scattering and ultrasound experiments [29].

In Ref. [4] it was found that in the case of $Sn_2P_2S_6$ crystal the dependence of energy as the function of local ferroelectric distortion requires polynomial expansion up to the 16th power. Recently, phenomenological modeling in $Sn_2P_2Se_6$ revealed that the known thermodynamic anomalies in the IC phase above the lock-in PT at T_c could be properly described only when high-power expansion is taken into account, which reflects the high nonlinearity of the local potential [5,6].

Below T_c, in the ferroelectric phase, theoretical and experimental studies of the inhomogeneity of spontaneous polarization revealed typical width of the domains about several tens of micrometers [3]. The temperature variation of the domain structure also reveals some metastability [30], as was predicted by *ab initio* based effective Hamiltonian Monte Carlo simulations [4].

Recent high-precision heat diffusion experiments [31] performed in the vicinity of the LP under conditions of very slow cooling/heating rates of order of 10 mK/min revealed that critical exponents in paraelectric and ferroelectric phases, as well as ratio of amplitudes, are well described by the LP theory, where long-range dipole interactions are not accounted. This observation is related to significant screening of dipole interactions in $Sn_2P_2Se_6$ with relatively small fundamental band gap, and therefore, significantly high concentration of free charge carriers. Moreover, an interesting phenomenon was observed: experiments also revealed thermal hysteresis in T_c already for concentrations $x = 0.26$ (i.e., $x < x_{LP}$), where transition is expected to be purely second order.

This hysteresis can be understood as described in the following. When approaching to the LP two spatial modulations with a similar mesoscopic scale appear: (i) for the modulation period of IC phase, which is determined by interatomic interactions, and (ii) for the domain width in ferroelectric phase, that additionally depends on macroscopic conditions. Therefore, one can expect a significant interplay of these spatial modulations as a pinning of the domain structure by incommensurate wave of polarization (and vice versa), leading to a nonequilibrium phenomena in nearest vicinity of the LP.

In this paper, we study the dependence of dielectric and acoustic properties of $Sn_2P_2Se_6$ mixed crystals on different cooling rates. We will show that both incommensurate second-order (at T_i) and lock-in first-order (at T_c) transitions are still observed for $x = 0.28$ sample, when the lowest cooling rate of 0.002 K/min is fulfilled. This means that the LP concentration

coordinate is expected at smaller selenium content, probably near $x = 0.26$. The lock-in transition anomaly disappears when the cooling rate rises up to 0.1 K/min. Therefore, we point out that determination of the LP coordinates is affected by conditions of the experimental investigations.

The remainder of this paper is organized as follows: In Sec. II we describe experimental details of our study, Sec. III contains results of dielectric measurements, ultrasound, and Brillouin scattering experiments, and in Sec. IV we discuss obtained experimental results. We conclude in Sec. V.

II. EXPERIMENTAL DETAILS

We performed accurate study of dielectric susceptibility, ultrasound velocity, and Brillouin scattering. Special attention was paid to control temperature. The dielectric susceptibility was investigated utilizing digital Goodwill LCR-815 high-end LCR meter at frequency 10 kHz. Variation of temperature was in the range 0.1 to 0.002 K/min.

The measurements of the ultrasound velocity were performed using computer-controlled pulse-echo equipment [32]. The precision of relative velocity measurements was better than 10^{-4}. Temperature stabilization in ultrasound experiments was better than 0.02 K. The sample was carefully polished to have precisely parallel faces (001). Silicone oil was used as the acoustic coupling medium for longitudinal waves. The measurements were carried out at 10-MHz frequency, using piezoelectric $LiNbO_3$ transducers.

The Brillouin scattering was investigated in backscattering geometry using a He-Ne laser and a pressure-scanned three-pass Fabry-Pérot interferometer [29] with sharpness of 35 and free spectral range of 2.51 cm^{-1}. The samples were placed in a UTREX cryostat in which the temperature was stabilized with an accuracy of 0.3 K.

Single crystals of the $Sn_2P_2(Se_xS_{1-x})_6$ were grown by the vapor transport (VT) and Bridgeman (BR) technologies. The content of sulfur and selenium in obtained samples is in good agreement with their nominal values [15,33]. All investigated samples were prepared as plates with $5 \times 5 \times 3$ mm^3 dimensions. Silver paste electrodes were attached to the largest (001) face, which is nearly normal to the direction of spontaneous polarization.

III. RESULTS

The temperature dependence of dielectric susceptibility for $Sn_2P_2(Se_xS_{1-x})_6$ crystals, that were grown by VT method, are shown on Fig. 1. For the samples with compositions $x = 0$, 0.22, and 0.28, the dielectric susceptibility at $T_0(x)$ has reached its maximal value of about 8000. For mixed crystal with $x = 0.4$ the maximum of susceptibility is smaller: it reaches its maximum of only near 6000. For $Sn_2P_2Se_6$ two dielectric anomalies are seen: with maximal susceptibility of about 3000 at T_c and about 1500 at T_i.

For $Sn_2P_2S_6$ and $Sn_2P_2Se_6$ crystals, grown by BR technology, the dielectric susceptibility in paraelectric phase obeys Curie-Weiss temperature dependence with Curie constant $C = (0.6–0.7) \times 10^5$ K. The susceptibility reaches very high values (above 10^5) at ferroelectric second-order transition (T_0) in sulfide compound and near 3×10^4 at first-order lock-in

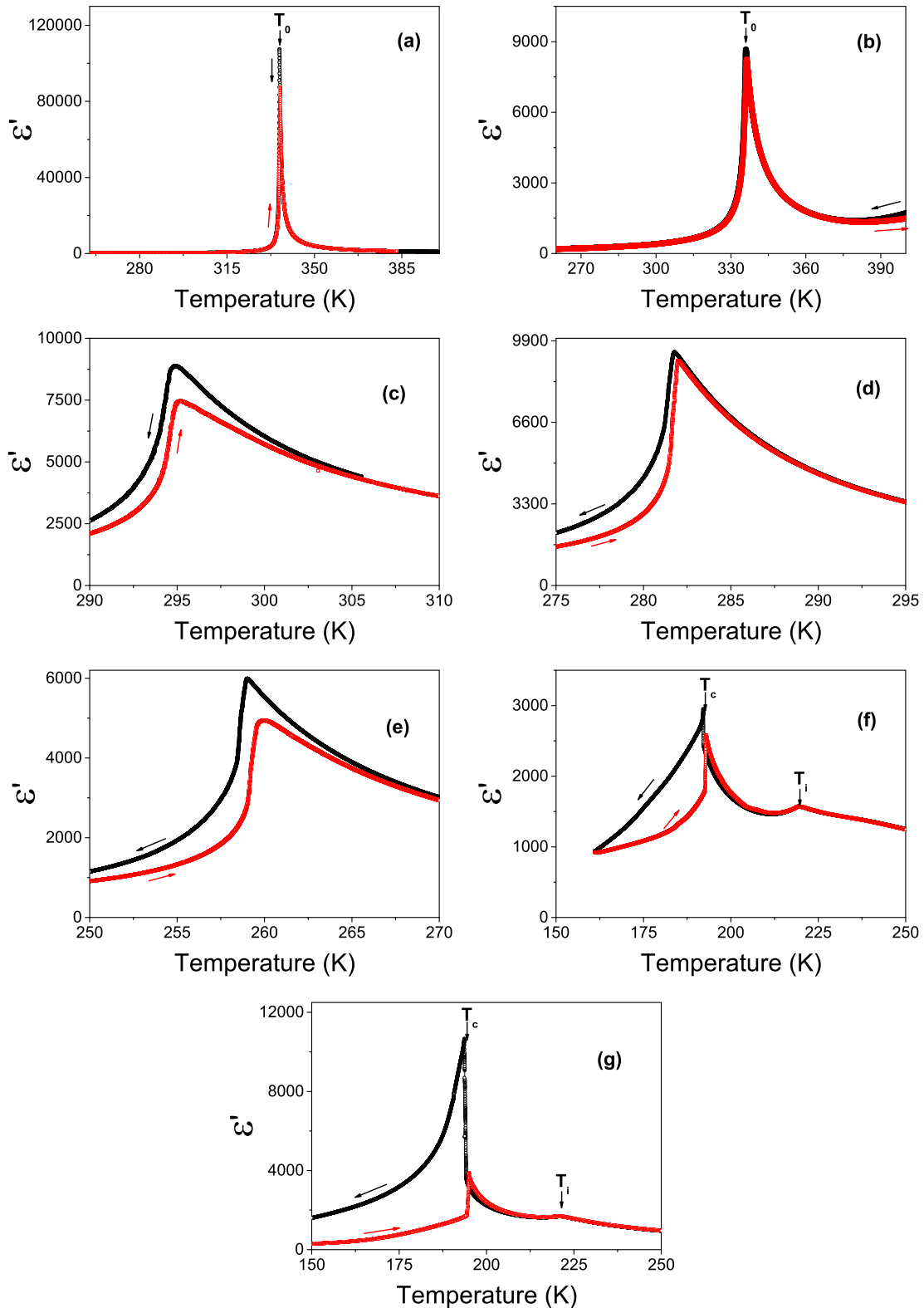FIG. 1. Temperature dependencies of dielectric susceptibility for $Sn_2P_2(Se_xS_{1-x})_6$ crystals measured at 0.005 K/min cooling and heating rate. (a) $x = 0$, BR sample; (b) $x = 0$, VT sample; (c) $x = 0.22$, VT sample; (d) $x = 0.28$, VT sample; (e) $x = 0.4$, VT sample; (f) $x = 1$, VT sample; (g) $x = 1$, BR sample.

transition T_c in selenide crystal (see Fig. 1). The difference in observed maxima of dielectric susceptibility in VT and BR samples is related to different contribution of domain walls to dielectric susceptibility in samples with different

conductivity: VT samples are more conductive [34]. Also, observed temperature hysteresis is related to contribution of domain walls. For the slow variation of temperature (0.005 K/min) the hysteresis in the position of maxima by

cooling and heating is about 0.2 K for the BR sample and it is somewhat larger (about 0.25 K) for the VT $Sn_2P_2S_6$ sample. For $Sn_2P_2Se_6$ selenide, the temperature hysteresis of the maxima of dielectric susceptibility at first-order lock-in transition (T_c) is about 1 and 2 K for VT and BR $Sn_2P_2Se_6$ samples, correspondingly.

The temperature hysteresis inside the IC phases of BR and VT $Sn_2P_2Se_6$ samples does not demonstrate such evident difference as in the case of domain-wall dielectric contribution. Temperature hysteresis is not observed for the paraelectric-to-IC transition (T_i) for both VT and BR $Sn_2P_2Se_6$ samples.

In any case, the dielectric behavior near the lock-in transition in $Sn_2P_2Se_6$ crystals is strongly dependent on the regime of measurements. The temperature width ΔT_c of the lock-in transition increases from 0.002 K at the cooling rate 0.005 K/min to 0.13 K at the rate 0.1 K/min, and further to 0.19 K at the rate 0.5 K/min [see Fig. 2(b)]. The dielectric susceptibility in the ferroelectric phase, for example, at 0.5 K below T_c [see Fig. 2(b)], also grows rapidly when cooling rate increases from 0.005 to 0.1 K/min. For higher rates, the dielectric susceptibility is almost constant.

These data demonstrate that the growth of the dielectric susceptibility at T_c is induced by the increase of the contribution of domain walls at higher cooling rates. Some increase of dielectric susceptibility in the low-temperature range of the incommensurate phase [see Fig. 2(a), together with widening of the lock-in transition temperature interval on Fig. 2(b)] could be also related to higher concentration of the modulation wave defects. These defects are areas with a new modulation period (so-called nucleations or stripples, see Refs. [35,36]), which appeared at faster cooling.

Naturally, the following question appears: What is the influence of the cooling rate on dielectric properties across the incommensurate phase with small temperature interval and with weak first-order lock-in transition in the nearest vicinity of LP? In this vicinity, the modulation wave period is large and could be comparable with the size of domains in the ferroelectric phase just below T_c. When the cooling rate increases, the concentration of the domain walls could also increase [37,38]. This allows the possibility that the size of domains will be near or equal to the IC modulation wavelength. Therefore, IC modulation wave could be pinned to the domain structure. This pinning will be observed experimentally as smeared anomalies of dielectric susceptibility in the vicinity of the LP. It is known that near the LP the phase transition lines $T_i(x)$ and $T_c(x)$ (which are the borders of the incommensurate phase) must tangentially coincide with the $T_0(x)$ line of direct transition from the paraelectric phase into ferroelectric one [8]. Therefore, the correct phase diagram in the vicinity of the LP can be obtained only at experimental conditions which are close to equilibrium. In real experiments, such conditions could be satisfied by sufficiently slow variation of temperature, especially in the cooling regime. To achieve these conditions we have investigated acoustic properties of $Sn_2P_2(Se_xS_{1-x})_6$ with high resolution in temperature changes and temperature behavior of dielectric susceptibility at the cooling (heating) rates slowed down to 0.002 K/min.

For the beginning we generalize available data about the temperature-concentration $T - x$ phase diagram for the $Sn_2P_2(Se_xS_{1-x})_6$ mixed crystals. Our new data concerning the

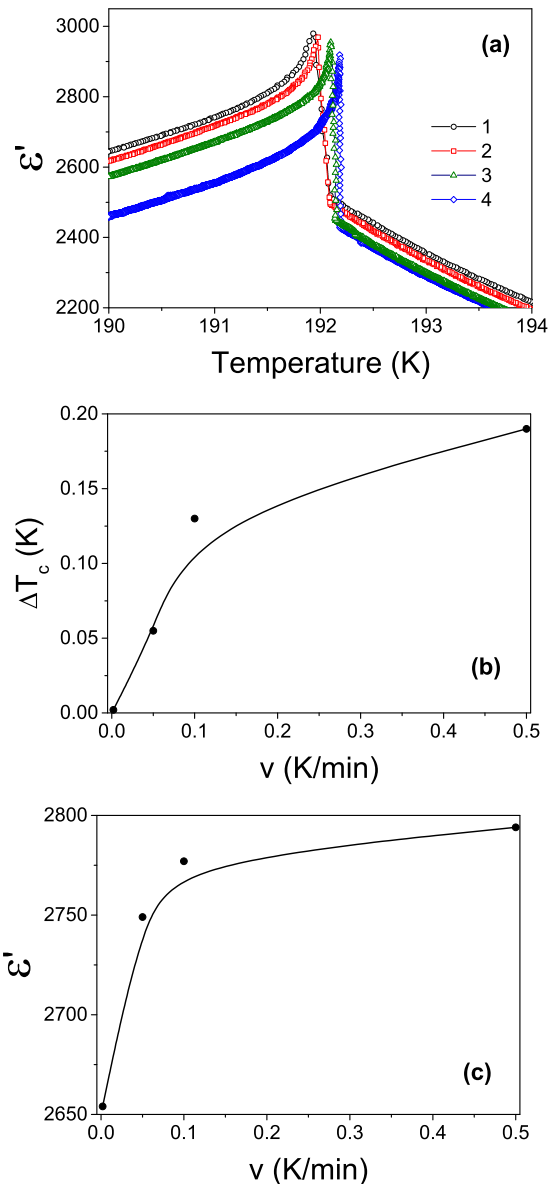

FIG. 2. (a) Temperature dependence of dielectric susceptibility for $Sn_2P_2Se_6$ VT sample at the following cooling rates: (1) 0.5 K/min, (2) 0.1 K/min, (3) 0.05 K/min, and (4) 0.005 K/min. The cooling rate dependencies of the (b) lock-in transition temperature width and (c) dielectric susceptibility at $T_c - 0.5$ K. The lines on (b) and (c) are a guide for the eye.

temperature positions of dielectric anomalies are compared with known data obtained in various experiments. Previously, the phase transitions in $Sn_2P_2(Se_xS_{1-x})_6$ crystals were investigated by optical absorption [33], x-ray diffraction [13,15], neutron scattering [14], heat capacity [39], heat diffusion [31], Brillouin scattering [24,29], ultrasound [29,32], and dielectric susceptibility [40] measurements. The $T - x$ diagram, that includes a large set of available experimental data, is presented in Fig. 3. This diagram indicates at $x_{LP} \sim 0.28$ the presence of a triple point (namely, the LP), at which the line $T_0(x)$ of second-order phase transitions from paraelectric to ferroelectric phases is continuously split into line $T_i(x)$ of the second-order transitions and line $T_c(x)$ of the first-order transitions. Between these lines the IC phase is observed. The wave
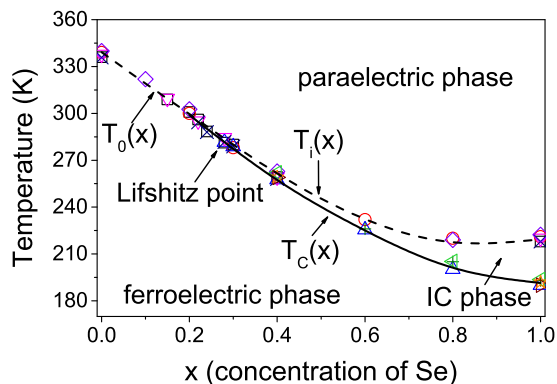
FIG. 3. Phase diagram of $Sn_2P_2(Se_xS_{1-x})_6$ ferroelectrics. The second-order paraelectric-ferroelectric $T_0(x)$ (at $x < x_{LP}$) and paraelectric-IC $T_i(x)$ (at $x > x_{LP}$) transitions are shown by the dashed line. By the solid line the first-order lock-in transitions between IC and ferroelectric phases are presented. Different style points present experimental data for the transitions temperatures T_0, T_i, and T_c: □, Refs. [31,44] (thermal diffusivity, T_0, T_i); ▷, Ref. [31] (thermal diffusivity, T_c); ○, Refs. [13,15] (x-ray diffraction, T_0, T_i); +, Ref. [15] (x-ray diffraction, T_c); ×, Refs. [34,40] (dielectric susceptibility, T_0, T_i); △, Ref. [34] (dielectric susceptibility, T_c); ▽, Refs. [29,32] (ultrasound, T_0, T_i); ☆, Ref. [32] (ultrasound, T_c); ◇, Ref. [39] (heat capacity, T_0, T_i); ◁, Ref. [39] (heat capacity, T_c).

number of incommensurate modulation q_i, which appears along the $T_i(x)$ line, decreases when the LP is approached. The concentration dependencies [15] of the IC phase temperature width $T_i - T_c$ and modulation wave number q_i (see Fig. 4) could be interpolated by relations $T_i - T_c \sim (x - x_{LP})^2$ and $q_i \sim (x - x_{LP})^{0.5}$, in agreement with predictions made by the mean field theory [8]. In the case of one component order parameter and one direction of the IC modulation, an inflection of the border line of paraelectric phase at the LP [7,8] is expected. Therefore, one could expect different curvatures for the $T_0(x)$ and $T_i(x)$ segments. Indeed, from the polynomial fitting for all sets of experimental data on T_0 and T_i values in $Sn_2P_2(Se_xS_{1-x})_6$ crystals, such inflection is clearly seen (see Fig. 5), and the inflection point is placed near $x = 0.22$.
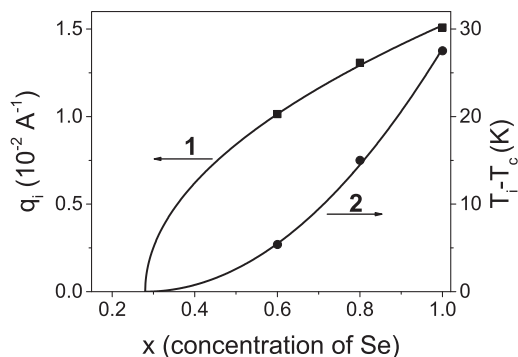

FIG. 4. The concentration dependencies of the modulation wave number along $T_i(x)$ line (1) and temperature width $T_i - T_c$ of IC phase (2) for $Sn_2P_2(Se_xS_{1-x})_6$ crystals. Points denote experimental data from Ref. [15]. Lines denote the fit by relations $q_i \sim (x - x_{LP})^{0.5}$ and $T_i - T_c \sim (x - x_{LP})^2$.

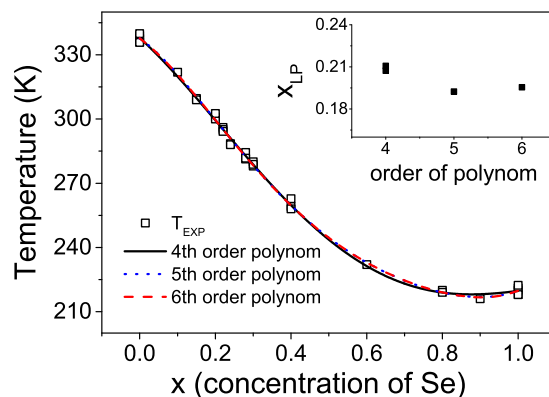FIG. 5. Fitting of $T_0(x)$ (at $x < x_{LP}$) and $T_i(x)$ (at $x > x_{LP}$) phase transition lines on $Sn_2P_2(Se_xS_{1-x})_6$ diagram by polynomials of fourth, fifth, and sixth order. By squares the experimental data for T_0 and T_i (from Fig. 4) are shown. Inset: the inflexion point concentration (that could be related to the LP concentration) in dependence of polynomial order.

The position of the LP could also be evaluated from the evolution of the temperature dependence of phonon spectra at different concentration x. Previously, neutron scattering study [14] revealed linear interaction of low-energy soft optic and acoustic phonon branches in $Sn_2P_2Se_6$ crystal. This interaction was phenomenologically described as a Lifshitz-type invariant in the thermodynamic potential function for proper uniaxial ferroelectrics with type II IC phase [14,16,25–27]. Such linear interaction near the LP results in a softening of acoustic phonons, which have been observed for the $Sn_2P_2(Se_xS_{1-x})_6$ crystals in Brillouin scattering and ultrasound investigations [29]. Naturally, one could expect that the acoustic branches softening in some part of reciprocal space near the Brillouin zone center will be reflected in the phonon contribution to the thermal transport. Indeed, according to the thermal diffusion data [31], the thermal conductivity in the paraelectric phase of $Sn_2P_2(Se_xS_{1-x})_6$ crystals lowers when sulfur is substituted by selenium (see Fig. 6). But, such lowering occurs only until concentration of selenium reaches $x = 0.22$, which is
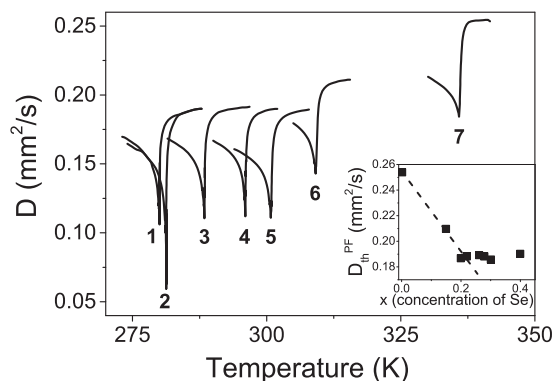

FIG. 6. Temperature anomalies of heat diffusion coefficient in $Sn_2P_2(Se_xS_{1-x})_6$ crystals with (1) $x = 0.30$, (2) $x = 0.28$, (3) $x = 0.26$, (4) $x = 0.22$, (5) $x = 0.20$, (6) $x = 0.15$, (7) $x = 0$, according to data from Ref. [31]. Inset illustrates concentration dependence of heat diffusion coefficient in the paraelectric phase.
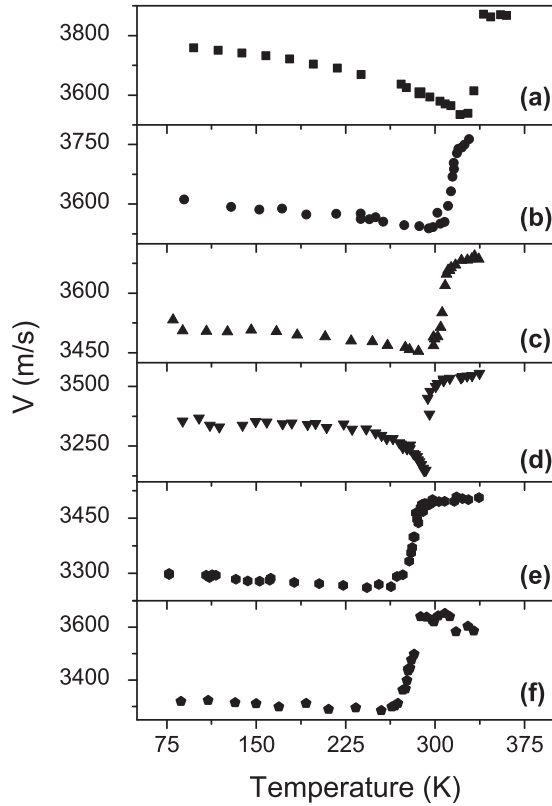
FIG. 7. Temperature dependence of longitudinal hypersound velocity obtained by Brillouin scattering in Z(X X)-Z geometry for $Sn_2P_2(Se_xS_{1-x})_6$ mixed crystals with (a) $x = 0$, (b) $x = 0.10$, (c) $x = 0.15$, (d) $x = 0.22$, (e) $x = 0.28$, (f) $x = 0.30$.

FIG. 8. Temperature variation of longitudinal ultrasound velocity at phase transition in $Sn_2P_2(Se_xS_{1-x})_6$ crystals with (1) $x = 0.4$, (2) $x = 0.28$, (3) $x = 0.15$, (4) $x = 0$. Inset illustrates concentration dependence of hypersound velocity in the paraelectric phase according to data from Fig. 7.

The IC phase broadening is clearly observed [31] in the heat diffusion anomaly for the sample with $x = 0.4$ composition [see Fig. 9(b)]. Our ultrasound data for the same composition $x = 0.4$ [Fig. 9(a)] show that the temperature anomalies of sound velocity in cooling and heating regimes are very similar to the heat diffusion anomalies in similar regimes. Here, the temperature hysteresis about 0.3 K [see Fig. 9(b)] appears, which is an evidence of rather strong first-order lock-in transition at T_c. This hysteresis is comparable with

smaller than the expected selenium content in mixed crystal with the LP composition $x_{LP} \sim 0.28$. Such peculiarity could be explained by the fact that in the heat transport the short-length phonons are dominated because they have relatively high concentration (i.e., high density of states) and high group velocity. Therefore, softening of acoustic phonons in the narrow vicinity of the LP does not influence the thermal transport.

Results of our Brillouin scattering investigations are presented on Fig. 7 as the temperature dependence of the hypersound velocity. For $Sn_2P_2(Se_xS_{1-x})_6$ mixed crystals, the temperature dependence of longitudinal hypersound in [001] direction is similar to recently reported [24,29] compositions $x = 0$ and 0.28. Here, we present results for an extended set of compositions to determine concentration dependence of hypersound velocity in the paraelectric phase. It appears that such velocity reaches its minimal value near the expected composition $x_{LP} = 0.28$.

The deepest minimum in the temperature dependence of ultrasound speed is observed at the composition $x = 0.28$, which is related to the LP position (see Fig. 8). Similar deepest minimum in the temperature dependence of heat diffusion was observed exactly at $x = 0.28$ in $Sn_2P_2(Se_xS_{1-x})_6$ mixed crystals [31] (compare with Fig. 6). For $x = 0.3$ composition, the anomaly of ultrasound velocity becomes shallower due to temperature hysteresis of the IC phase and first-order lock-in transition.
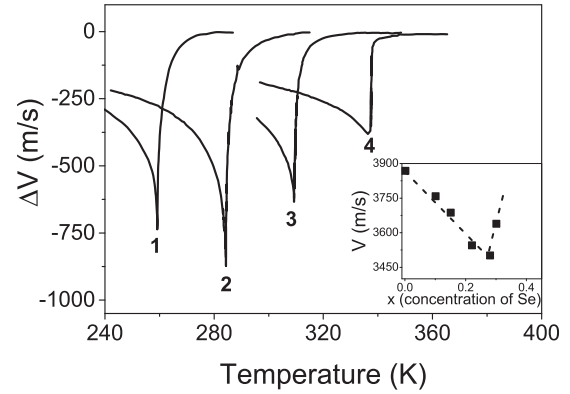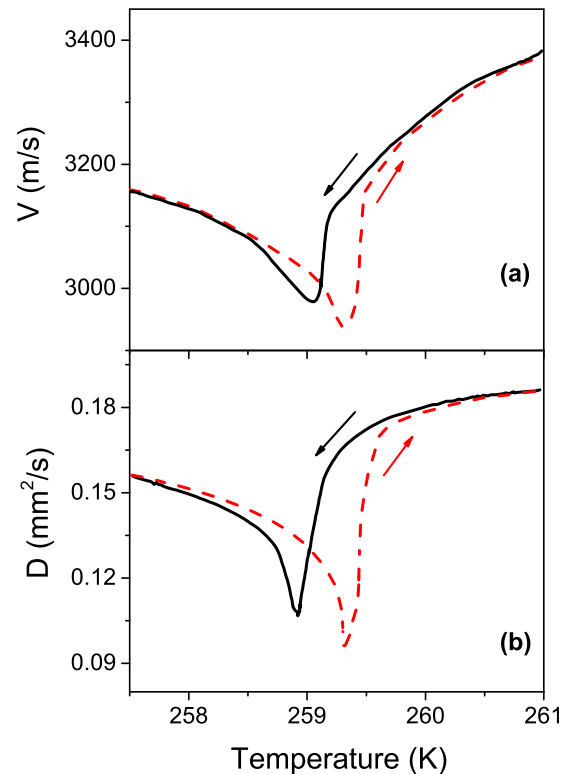

FIG. 9. Temperature dependence of (a) longitudinal ultrasound velocity, and (b) heat diffusion coefficient [31] by cooling and heating across the phase transitions in $Sn_2P_2(Se_xS_{1-x})_6$ crystals with $x = 0.4$.
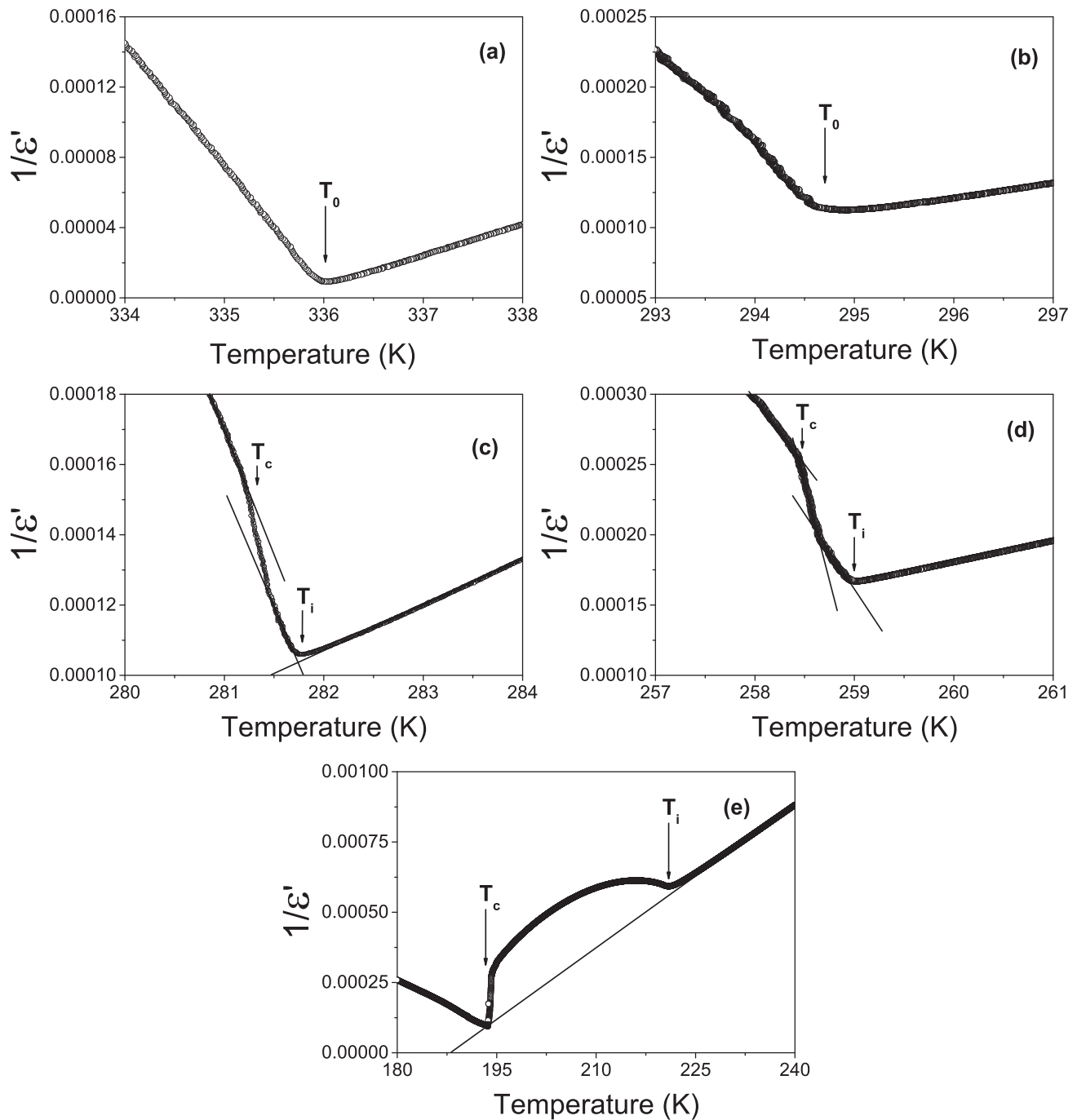
FIG. 10. Temperature dependence of reciprocal dielectric susceptibility at 0.005 K/min cooling rate for $Sn_2P_2(Se_xS_{1-x})_6$ mixed crystals with (a) $x = 0$, (b) $x = 0.22$, (c) $x = 0.28$, (d) $x = 0.4$, (e) $x = 1$.

the temperature interval of the IC phase $T_i - T_c$ for this composition.

In general, the acoustic data (which provide information about phase velocity of the ultrasound or hypersound waves) and heat diffusion data (which characterize group velocity of the short-waves phonons), together with general shape of $T - x$ diagram for $Sn_2P_2(Se_xS_{1-x})_6$ mixed crystals (which is based on wide set of different experiments), give an evidence that the LP should be placed at selenium concentration smaller than $x = 0.28$, somewhere in the interval of $0.22 < x < 0.28$.

Further, we will discuss the high-precision dielectric data, that could help to localize the LP and check possible nonequilibrium effects in their vicinity. Clear Curie-Weiss behavior is observed in reciprocal dielectric susceptibility in both paraelectric and ferroelectric phases of $Sn_2P_2S_6$ crystal with second-order PT at T_0 (see Fig. 10). For $Sn_2P_2Se_6$ crystal, the Curie-Weiss behavior is seen only in the paraelectric phase. Almost symmetric maximum of $1/\epsilon(T)$ dependence is related to continuous PT ($T_i \sim 221$ K) from paraelectric into IC phase. Clear discontinuity in dielectric susceptibility occurs
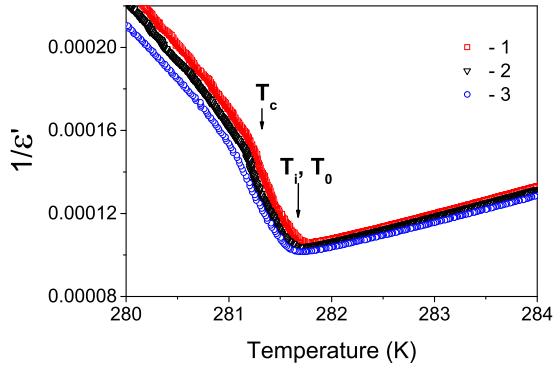
FIG. 11. Temperature dependence of reciprocal dielectric suscep-
tibility for $Sn_2P_2(Se_xS_{1-x})_6$ mixed crystal with $x = 0.28$ at different
cooling rates: (1) 0.005 K/min; (2) 0.05 K/min; and (3) 0.1 K/min.

at first-order lock-in transition ($T_c \sim 193$ K). From these data
it follows that in the selenide compound, the IC phase is
ranged in temperature interval $T_i - T_c \sim 28$ K. For mixed
crystals, the nonmonotonic behavior in $1/\epsilon(T)$ dependence
is also observed, which could be used to define the borders
of IC phase with temperature width $T_i - T_c$ near 0.7 K for
$x = 0.4$ sample and near 0.25 K for $x = 0.28$ sample. In case
of $x = 0.22$ mixed crystal, the dependence $1/\epsilon(T)$ already
shows Curie-Weiss behavior in paraelectric and ferroelectic
phases with some jump in ferroelectric phase just below T_0 (see
Fig. 10). So, at low cooling rate the IC phase is clearly observed
for the $x = 0.4$ mixed crystal and in very small temperature
interval also for $x = 0.28$ sample. But, at faster cooling the
jump on $1/\epsilon(T)$ dependence smears for this sample ($x = 0.28$)
(see Fig. 11) and dielectric anomaly becomes similar to the one
found in the case of $x = 0.22$ concentration.

IV. DISCUSSION OF EXPERIMENTAL DATA

First, let us analyze the phase diagram near the LP
(Fig. 3). As it was mentioned above, for one component
order parameter the mean field approximation predicts [8] that
the temperature interval of the IC phase has parabolic con-
centration dependence $T_i - T_c \sim (x - x_{LP})^2$. With account of
fluctuation effects, the phase diagram is described by critical
index $\Phi = 0.625$ in relation $T_i - T_c \sim (x - x_{LP})^{\frac{1}{\Phi}}$ [22,23].
It is seen that in the mean field approximation, $\Phi = 0.5$.
Also, the concentration behavior of modulation wave number
q_i along the $T_i(x)$ transition line follows the relation $q_i \sim
(x - x_{LP})^{\beta_q}$ with index $\beta_q = 0.5$ in the mean field approach
[8]. The critical behavior near the LP in uniaxial ferroelectrics
could be modified by long-range dipole interactions [17].
Also, possible proximity to the tricritical LP point is re-
flected in the new universality class in uniaxial ferroelectrics
[18–20].

Recent heat diffusion investigations [31] point out that
the Lifshitz point in $Sn_2P_2(Se_xS_{1-x})_6$ mixed crystals is
located near $x = 0.28$. The critical exponents and ratio of
the critical amplitudes of heat capacity in paraelectric and
ferroelectric phases satisfy predicted critical behavior at the
LP in systems without long-range interactions [31]. Such
peculiarity was related to possible screening of dipole-dipole

interactions in semiconducting $Sn_2P_2(Se_xS_{1-x})_6$ with small
band gap [31]. True critical behavior is observed in very
narrow (8×10^{-3} to 5×10^{-5}) range of reduced temperature
$(T - T_0)/T_0$, or in temperature interval $T - T_0$ from 2.4 to
0.015 K relative to the transition temperature T_0. In case
of $Sn_2P_2S_6$ crystals, the critical behavior for birefringence
[42], dielectric susceptibility [43], ultrasound velocity [41],
and heat capacity on thermal diffusion data [44] satisfies the
mean field exponents with small multiplicative logarithmic
corrections [20]. Therefore, we could expect that for analysis
of the $T - x$ diagram in $Sn_2P_2(Se_xS_{1-x})_6$ mixed crystals,
the mean field values $\Phi = 0.5$ and $\beta_q = 0.5$ should be
appropriate.

According to the experimental data (see Fig. 3) for the
selenium compound ($x = 1$), the temperature difference $T_i -
T_c$ is ∼28 K. As it was discussed above, the LP has position at
$x = 0.28$ or at a bit smaller selenium concentration.

Using the relation $T_i - T_c \sim (x - x_{LP})^2$ one could estimate
that for the mixed crystal with chemical content $x = 0.4$ the
temperature width of IC phase $T_i - T_c$ is equal to 0.78 K.
If we assume that the LP is located at $x_{LP} = 0.26$, similar
estimation gives the temperature interval $T_i - T_c$ equal to 1 K
for the same concentration $x = 0.4$. Therefore, for the sample
with $x = 0.28$ the IC phase is predicted to be observed in very
small temperature range $T_i - T_c = 0.02$ K.

From the temperature anomalies in dielectric susceptibility
(see Fig. 10), it follows that temperature interval of the IC phase
is about 0.6 K for $x = 0.4$ and is about 0.2 K for $x = 0.28$.
Experimentally observed temperature range of the IC phase for
$x = 0.4$ is obtained, when we assume the LP coordinate to be
$x_{LP} = 0.28$. However, much wider experimentally observed
temperature range (about 0.2 K) of the IC phase for the
$x = 0.28$ sample does not agree with such estimations. The
estimated interval $T_i - T_c$ reaches the value of 0.17 K at
the $x = 0.28$ only if we assume that the LP is located at
$x_{LP} = 0.22$.

As it follows from the above-described estimations, for
the sample with $x = 0.4$ a true IC phase with temperature
width near 0.6 K is observed (see Fig. 10). In mixed crystal
with $x = 0.28$ an intermediate state between paraelectric and
ferroelectric phases is still observed, which obviously could
be related to some space interference of the long-period
modulation wave with regular domain structure with very
high concentration of domain walls. This space interference
is seen in temperature behavior of the reciprocal dielectric
susceptibility for the $x = 0.28$ sample at different cooling rates
(see Fig. 11): For the lowest rate 0.005 K/min, the mentioned
dependence is similar to the one observed for the $x = 0.4$
sample. For the highest rate 0.1 K/min, this dependence
becomes similar to the anomaly shape in the case of $x = 0.22$
sample (compare with Fig. 10).

As it was mentioned above, $Sn_2P_2S_6$ and $Sn_2P_2Se_6$ crystals
are proper uniaxial ferroelectrics. $Sn_2P_2Se_6$ has IC phase
with almost transverse long-wave modulation as a result of
specific interatomic interaction. This IC phase is not related
to the symmetry, therefore, the Lifshitz invariant is absent in
the thermodynamic functional. Here, the modulation in the
IC phase of type II is almost harmonic [45]. At least, any
evidences of higher harmonics were not found in the x-ray
and neutron diffraction experiments [13,14]. The first-order

lock-in transition between IC and ferroelectric phase was clearly observed [31,39].

At low-temperature edge of the IC phase, a temperature behavior of some thermodynamic properties (namely, heat capacity, dielectric susceptibility, heat expansion) deviates from the one predicted in the one-harmonic approximation. The discrepancies still exist even when the higher harmonics in the spatial modulation of the order parameter in the IC phase are taken into account. This was observed as a quantitative difference of calculated and experimental temperature behavior of thermodynamic properties and modulation wave number in the IC near the lock-in transition [46]. Only recently these experimental data have successfully been explained when higher-order invariants (including 8 and 10 powers), as well as biquadratic coupling of the order parameter with its space derivative, were accounted in the Landau functional [5,6]. Such explanation agrees well with strongly anharmonic three-well local potential of $Sn_2P_2S_6$-like ferroelectrics, which was obtained by *ab initio* study of their electronic and dynamical properties [4].

Strong nonlinearity of SPS ferroelectrics allows possibility of specific domain structure with wide domain walls, which include nonpolar regions [4,30]. In order to simulate the influence of the cooling rate on the configuration of the domains in $Sn_2P_2S_6$, we performed Monte Carlo studies of the effective three-well potential Hamiltonian obtained from the first-principles investigations [4]. This Hamiltonian depends on the amplitude of the local mode, which in our case describes atomic displacements of two low-energy optical modes: a polar B_u mode, for which the Sn cations are moved out of phase to the anionic $[P_2S_6]^{2-}$ complexes, and full-symmetry A_g mode, which describes out-of-phase displacements in the Sn sublattices. The effective Hamiltonian

explicitly accounts for the following interactions of the local modes: (i) a self-interaction, which in our case is strongly anharmonic (see discussion in Ref. [4]); (ii) short-range intercell interaction; (iii) long-range Coulomb interaction; (iv) elastic energy; and (v) anisotropic coupling of the local mode to elastic deformations. In Monte Carlo (MC) simulations, we used $1 \times 200 \times 1$ supercell. This means that we allowed evolution of the domains in crystallographic direction b (as it is observed experimentally), whereas in other directions we assumed mean field behavior. This effective Hamiltonian was solved in a cooling regime starting from 600 K with temperature steps of 5 K down to 10 K. Variations of the cooling rate were simulated by different numbers of pseudospin updates. In so-called *fast* cooling, we used 10^5 updates for each pseudospin both for equilibration and production cycles. *Slow* cooling was simulated by 10^6 updates. The temperature evolution of the domain structure at different cooling rates and several temperatures is shown in Fig. 12. It is clearly seen that in the vicinity of the phase transition temperature (∼337 K) domain configuration obtained in the *fast* regime reveals short-period microdomains. This is in contrast to the *slow* cooling, where resulted domain configuration is almost harmonic with the period of the simulation cell. The effect of the cooling rate on domain configuration is important only in the vicinity of the phase transition. Upon further cooling, the domain structure in both cases reveals two clearly distinguished areas with opposite directions of the polarization. Sharp domain walls with nonpolar areas are observed at very low temperatures.

We should note that similar exotic temperature evolution of the domain structure with high flexibility was recently predicted by MC simulation and consequently confirmed in piezoresponse force microscopy (PFM) experiments [30].
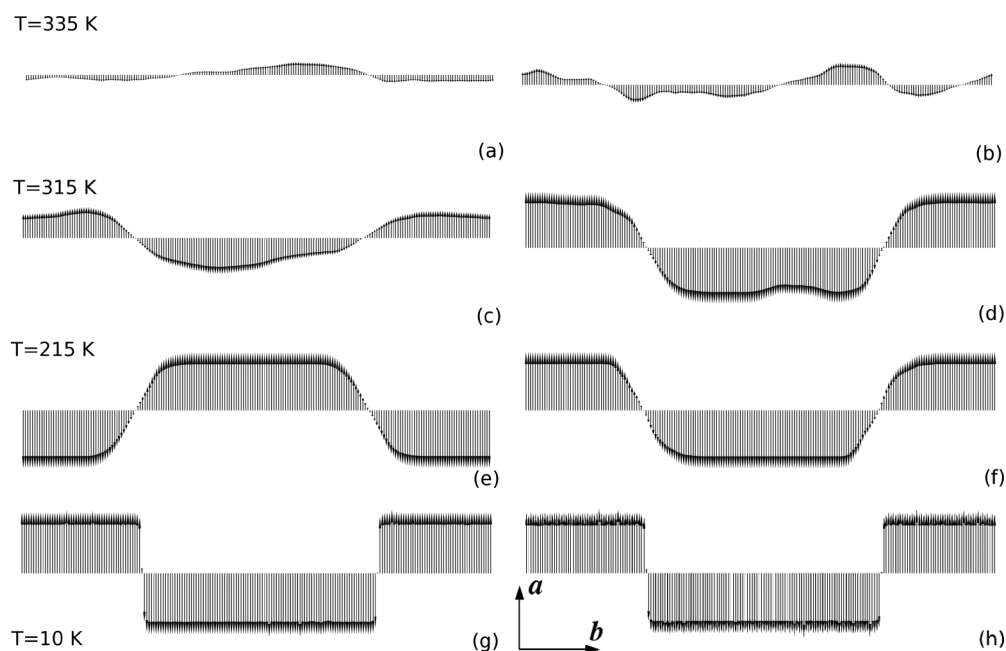

FIG. 12. Monte Carlo domain structure of $Sn_2P_2S_6$ at various temperatures and different length of Markov chains in cooling regime: (a), (c), (e), (g) correspond to 10^6 sweeps per pseudospin (and, correspondingly, *slow* cooling rate), whereas (b), (d), (f), (h) results are obtained for 10^5 sweeps per pseudospin (i.e., the *fast* cooling). Direction of the polarization is mostly along crystallographic period a. Domain structure appears along crystallographic direction b.

Increasing the domain-wall concentration by heating in ferroelectric phase was found in $Sn_2P_2Se_6$ crystal analytically and in phase-field modeling [3]. It seems that below the lock-in transition temperature T_c, the mean size of domains is small enough and the width of the domain walls is very significant, i.e., domain structure becomes similar to the periodically modulated space distribution of the spontaneous polarization in the IC phase. Possible similarity of the space distribution of spontaneous polarization just below T_c and above this temperature is also supported by the presence of small kink in the optic birefringence at lock-in transition in $Sn_2P_2Se_6$ [47]. High dielectric response of the domain walls below lock-in transition (see Fig. 1) is evidently also related to their high concentration.

When the LP is approached along $T_c(x)$ line, the modulation period of the IC phase increases and at certain conditions could become comparable with domain dimensions in the ferroelectric phase near the LP. Also, the temperature range $T_i - T_c$ of the IC phase disappears when approaching the LP. Obviously, just above T_c the modulation wave is expected to be harmonic. Some kink in dielectric properties at T_c near the LP is related to small difference in space profile of spontaneous polarization in IC and ferroelectric phases. The concentration of domain walls depends on the cooling rate. Therefore, the observed kink at T_c in the dielectric susceptibility could be changed, when the cooling rate is varied.

Next, we will try to discuss the domain wall in uniaxial ferroelectrics as the scalar topological defects. Indeed, in considered case of the transition from paraelectric phase with $2/m$ point group to ferroelectric one with m symmetry group, discrete change of symmetry occurs. At the same time, domains with opposite direction of spontaneous polarization are separated by domain walls where polarization passes through zero. These walls could be classified as 0-sphere or scalar topological defects [48]. According to Kibble-Zurek theory [37,38], concentration of such defects depends on the cooling rate across second-order transition from the paraelectric phase to the ferroelectric one. When a system goes through a symmetry-breaking phase transition (from a symmetric phase into one with spontaneously broken symmetry), the order parameter might make different choices in different regions, creating polar domains. Domains with different direction of polarization, when they meet, can create defects such as the domain walls. The scale of those domains, and hence the density of defects, is constrained by the speed at which the system goes through the transition and the speed with which order-parameter information propagates. At slow cooling rate, different regions can propagate their choice of phase: large regions found the same choice and low density of defects is presented. At fast cooling rate, there is less time to communicate the choice of phases. Therefore, many small regions with different choice of phases appear, i.e., density of defects is high.

When Kibble-Zurek theory was applied to ferroelectrics, it was argued [49] that for fast cooling through the phase transition point, the distance over which information can be transferred is short and becomes equal to the smallest correlation length $\xi(T)$. Therefore, freeze-out occurs when the domain size is small and, consequently, the concentration of topological defects, which are domain walls n_w, is large.

In contrast, for slow cooling, the distance for information transfer is large and does not become equal to $\xi(T)$ until the phase transition temperature is reached, where $\xi(T)$ is large. In this case, large domains are formed, and a few topological defects such as domain walls are observed. Quantitatively, the Kibble-Zurek theory predicts the following dependence of domain size d on cooling speed [37,38]:

$$d = \xi_0 \left(\frac{\tau_q}{\tau_0} \right)^{\frac{\nu}{1+\mu}}, \qquad (1)$$

where ξ_0 is zero-temperature correlation length, that is proportional to the domain-wall width; $\tau_q = \frac{T_0}{\nu_T}$ is a ratio of the PT temperature T_0 to the cooling speed $\nu_T = \frac{dT}{dt}$; $\tau_0 = \frac{\xi_0}{\nu_s}$ is zero-temperature relaxation time, where ν_s is speed of sound. The critical indexes μ and ν determine divergence of correlation length and relaxation time at transition temperature:

$$\xi(T) = \xi_0 \left(1 - \frac{\tau}{\tau_0} \right)^{-\nu}; \quad \tau(T) = \tau_0 \left(1 - \frac{\tau}{\tau_0} \right)^{-\mu}. \qquad (2)$$

We employ these relations to estimate domain-wall concentration as a function of cooling rate across second-order transition from the paraelectric to ferroelectric phase in $Sn_2P_2S_6$ crystals. Here, we suppose that such estimation of domain-wall concentration is valid below the $T_0(x)$ line until the vicinity of LP. In the vicinity of the LP in uniaxial ferroelectrics $Sn_2P_2(Se_xS_{1-x})_6$ near the tricritical point on $T - x$ diagram [9,16], the universality class of the UTLP could be appropriated. Such polycritical point is described by mean field critical indexes with small multiplicative logarithmic corrections [20] and values $\nu = 0.5$ and $\mu = 1$ could be used for estimations. As follows from the DFT-based model Hamiltonian calculations [4], the width of the lowest-energy domain walls in $Sn_2P_2S_6$ crystals is about two unit cells, i.e., $\xi_0 \approx 20$ Å. The speed of transverse acoustic waves in the paraelectric phase was experimentally determined to be $\nu_s \approx 2200$ m/s for $Sn_2P_2S_6$ crystals and decrease to 2000 m/s in the mixed crystals with $x = 0.28$ [29].

With this set of parameters it follows from relation (1) that at cooling rate $\frac{dT}{dt} = 0.005$ K/min the domain size d is about 230 μm. When cooling rate is 0.1 K/min, the value of d lowers to ≈ 50 μm. We suppose that similar scale of domain structure just below the $T_0(x)$ line remains when concentration of selenium increases from 0 to $x_{LP} = 0.28$. Such scale is comparable with several micrometers modulation wavelength $\lambda_i = \frac{2\pi}{q_i}$ for $q_i \approx 10^{-3}$ Å^{-1} near the LP at concentration distance $x - x_{LP} \approx 0.01$ (see Fig. 4).

V. CONCLUSIONS

For $Sn_2P_2(Se_xS_{1-x})_6$ mixed crystals with selenium concentration near the the Lifshitz point $x_{LP} \sim 0.28$, the anomalies of dielectric susceptibility clearly revealed the existence of the incommensurate phase with the temperature interval, which depends on the cooling rates. Observed dependence of lock-in transition on the cooling rate could be associated with the transformation of the long-wave modulation of polarization into domain structure. Concentration of the domains is determined by strongly nonlinear local potential

and has different values depending on the cooling rate. For composition $x = 0.28$ in the regime of the slowest cooling rate 0.002 K/min, the intermediate IC phase has temperature interval between T_i and T_c of about 0.1 K. The kink in dielectric susceptibility at lock-in transition T_c smears by increasing the cooling rate to 0.1 K/min. This smearing is related to the corresponding increase of the domain-wall concentration n_w in the ferroelectric phase just below T_c. We suggest that n_w strongly increases when the cooling rate increases from 0.002 to 0.1 K/min. The highest estimated value of n_w gives a distance between the domain walls, which

is comparable with modulation wavelength for concentration $x \sim 0.29$.

[1] B.-K. Lai, I. Ponomareva, I. A. Kornev, L. Bellaiche, and G. J. Salamo, Phys. Rev. B **75**, 085412 (2007).

[2] E. A. Eliseev, S. V. Kalinin, Y. Gu, M. D. Glinchuk, V. Khist, A. Borisevich, V. Gopalan, L.-Q. Chen, and A. N. Morozovska, Phys. Rev. B **88**, 224105 (2013).

[3] A. N. Morozovska, E. A. Eliseev, J. J. Wang, G. S. Svechnikov, Y. M. Vysochanskii, V. Gopalan, and L.-Q. Chen, Phys. Rev. B **81**, 195437 (2010).

[4] K. Z. Rushchanskii, Y. M. Vysochanskii, and D. Strauch, Phys. Rev. Lett. **99**, 207601 (2007).

[5] V. Korda, S. Berezovsky, A. Molev, L. Korda, and V. Klepikov, Phys. B (Amsterdam) **407**, 3388 (2012).

[6] V. Korda, S. Berezovsky, A. Molev, L. Korda, and V. Klepikov, Phys. B (Amsterdam) **425**, 31 (2013).

[7] R. M. Hornreich, M. Luban, and S. Shtrikman, Phys. Rev. Lett. **35**, 1678 (1975).

[8] A. Michelson, Phys. Rev. B **16**, 5121 (1977).

[9] Y. M. Vysochanskii and V. Y. Slivka, Sov. Phys. Usp. **35**, 123 (1992).

[10] J. Hlinka, T. Janssen, and V. Dvorak, J. Phys.: Condens. Matter **11**, 3209 (1999).

[11] A. N. Rubtsov, J. Hlinka, and T. Janssen, Phys. Rev. E **61**, 126 (2000).

[12] G. H. F. van Raaij, K. J. H. van Bemmel, and T. Janssen, Phys. Rev. B **62**, 3751 (2000).

[13] T. K. Barsamian, S. S. Khasanov, V. S. Shekhtman, Y. M. Vysochanskii, and V. Y. Slivka, Ferroelectrics **67**, 47 (1986).

[14] S. W. H. Eijt, R. Currat, J. E. Lorenzo, P. Saint-Grégoire, S. Katano, T. Janssen, B. Hennion, and Y. M. Vysochanskii, J. Phys.: Condens. Matter **10**, 4811 (1998).

[15] T. K. Barsamian, S. S. Khasanov, and V. S. Shekhtman, Ferroelectrics **138**, 63 (1993).

[16] Yu. M. Vysochanskii, V. G. Furtsev, M. M. Khoma, A. A. Grabar, M. I. Gurzan, M. M. Maior, S. I. Perechinskii, V. M. Rizak, and V. Yu. Slivka, Zh. Eksp. Teor. Fiz. **91**, 1384 (1986) [Sov. Phys.–JETP **64**, 816 (1986)].

[17] R. Folk and G. Moser, Phys. Rev. B **47**, 13992 (1993).

[18] I. Nasser, A. Abdel-Hady, and R. Folk, Phys. Rev. B **56**, 154 (1997).

[19] I. Nasser, Phys. Rev. B **60**, 2983 (1999).

[20] R. Folk, Phase Transitions **67**, 645 (1999).

[21] W. Selke, Phys. Rep. **170**, 213 (1988).

[22] D. Baltrunas, R. Mikaitis, V. Y. Slivka, and Y. M. Vysochanskii, Phys. Status Solidi A **119**, 71 (1990).

[23] Y. M. Vysochanskii, D. Baltrunas, A. A. Grabar, K. Mazeika, K. Fedyo, and A. Sudavicius, Phys. Status Solidi B **246**, 1110 (2009).

[24] R. M. Yevych, Y. Vysochanskii, M. Khoma, and S. Perechinskii, J. Phys.: Condens. Matter **18**, 4047 (2006).

[25] A. Levanyuk and D. Sannikov, Fiz. Tverd. Tela **18**, 423 (1976) [Sov. Phys.–Solid State **18**, 245 (1976)].

[26] K. Ema, K. Hamano, and A. P. Levanyuk, J. Phys. Soc. Jpn. **59**, 1438 (1990).

[27] Y. Ishibashi and H. Shiba, J. Phys. Soc. Jpn. **45**, 409 (1978).

[28] S. Eijt, R. Currat, J. Lorenzo, P. Saint-Grégoire, B. Hennion, and Y. Vysochanskii, Eur. Phys. J. B **5**, 169 (1998).

[29] A. Kohutych, R. Yevych, S. Perechinskii, V. Samulionis, J. Banys, and Y. Vysochanskii, Phys. Rev. B **82**, 054101 (2010).

[30] D. A. Kiselev, K. Z. Rushchanskii, I. K. Bdikin, M. D. Malinkovich, Y. N. Parkhomenko, and Y. M. Vysochanskii, Ferroelectrics **438**, 55 (2012).

[31] A. Oleaga, A. Salazar, A. A. Kohutych, and Y. M. Vysochanskii, J. Phys.: Condens. Matter **23**, 025902 (2011).

[32] V. Samulionis, Ultragarsas **45**, 7 (2002).

[33] Y. Vysochanskii, T. Janssen, R. Currat, R. Folk, J. Banys, J. Grigas, and V. Samulionis, *Phase Transitions in Ferroelectric Phosphorous Chalcogenide Crystals* (Vilnius University Publishing, Vilnius, Lithuania, 2006).

[34] Y. M. Vysochanskii, A. A. Molnar, and M. M. Khoma, Ferroelectrics **223**, 19 (1999).

[35] K. Parlinski, Phys. Rev. B **39**, 12154 (1989).

[36] K. Parlinski, F. Dénoyer, and G. Eckold, Phys. Rev. B **43**, 8411 (1991).

[37] A. del Campo, T. W. B. Kibble, and W. H. Zurek, J. Phys.: Condens. Matter **25**, 404210 (2013).

[38] T. Kibble and G. Volovik, JETP Lett. **65**, 102 (1997).

[39] K. Moriya, H. Kuniyoshi, K. Tashita, Y. Ozaki, S. Yano, and T. Matsuo, J. Phys. Soc. Jpn. **67**, 3505 (1998).

[40] M. Maior, B. Koperles, Y. Vysochanskii, and M. Gurzan, Fiz. Tverd. Tela **26**, 690 (1984) [Sov. Phys.–Solid State **26**, 416 (1984)].

[41] V. Samulionis, J. Banys, Y. Vysochanskii, and A. A. Grabar, Phys. Status Solidi B **215**, 1151 (1999).

[42] Y. M. Vysochanskii, V. V. Mitrovcij, A. A. Grabar, S. I. Perechinskii, S. F. Motrja, and J. Kroupa, Ferroelectrics **237**, 193 (2000).

[43] A. A. Molnar, Y. M. Vysochanskii, A. A. Horvat, and Y. S. Nakonechnii, Ferroelectrics **192**, 137 (1997).

[44] A. Oleaga, A. Salazar, M. Massot, and Y. M. Vysochanskii, Thermochim. Acta **459**, 73 (2007).

[45] A. D. Bruce, R. A. Cowley, and A. F. Murray, J. Phys. C: Solid State Phys. **11**, 3591 (1978).

[46] M. Khoma, A. Molnar, and Y. Vysochanskii, J. Phys. Stud. **2**, 524 (1998).

[47] I. M. Rizak, V. M. Rizak, S. I. Perechinsky, Y. M. Vysochansky, and V. Y. Slivka, Ferroelectrics **143**, 67 (1993).

[48] T. W. B. Kibble, J. Phys. A: Math. Gen. **9**, 1387 (1976).

[49] S. M. Griffin, M. Lilienblum, K. T. Delaney, Y. Kumagai, M. Fiebig, and N. A. Spaldin, Phys. Rev. X **2**, 041022 (2012).